DOI 10.1007/s10891-017-1676-9

Journal of Engineering Physics and Thermophysics, Vol. 90, No. 5, September, 2017

TRANSFER PROCESSES IN RHEOLOGICAL MEDIA

ON THE APPLICABILITY OF THE OSTWALD–DE WAELE MODEL IN SOLVING APPLIED PROBLEMS

V. M. Shapovalov

UDC 532.135+536.24

By comparing the results of calculation of power-law fluid flow in a slit with the Ellis fluid flow, the inaccuracy of the power-law model is shown as much in describing the velocity profile as in determining the non-Newtonian fluid flow rate. Moreover, the error of the power-law model in the description of temperature distribution in the case of dissipative heating of non-Newtonian fluid over a stabilized segment is shown. The boundary condition of first kind was used.

Keywords: *flow rate, shear stress, pressure, rheological model, temperature, velocity.*

Introduction. For describing the section of variable viscosity of non-Newtonian fluids, de Waele (1923) and Ostwald (1925) suggested an empirical equation known as a power law. The Ostwald–de Waele model is widely used for describing flows of rheologically complex fluids (melts and polymer solutions) in technological equipment during the processing of these fluids. This is due to the relative simplicity of the two-parameter model and to the convenience of determining the rheological characteristics from the flow curve [1]. The main drawback of the power-law model is the error in describing the fluid behavior in the vicinity of low rates of deformation (of the highest Newtonian viscosity) [2].

Usually, a researcher, when constructing, for example, a model of flow in a channel, gives preference to the power-law model due to the following considerations. The highest shear rate (or shear stress) is near the channel wall. It corresponds to the portion of approximation of the flow curve. Precisely this region determines the behavior of flow, including the integral parameters. In the vicinity of the velocity maximum, the shear rate is close to zero. Under these conditions, the power-law model yields an overestimated effective viscosity for pseudoplastics. But the dimensions of the zone of high viscosity are insignificant, and this zone must not exert a substantial influence on flow. However, as will be shown below, the magnitude and the distribution of the effective viscosity in the "core" exert a substantial influence on the velocity profile, also in the "zone of gradient flow."

In the present work, an attempt has been made to estimate the error of application of the power-law model in solving the problems of flow and heat transfer in a plane channel. The estimate was obtained by comparing the calculated results for the power-law model with the results for an Ellis fluid. The Ellis model has been taken as a standard, since it gives a good description for the behavior of rheologically complex fluids at low and mean deformation rates. The three-parameter Ellis model at low shear rates predicts the Newtonian behavior of a fluid and the existence of the final viscosity value.

Non-Newtonian Fluid Flow in a Plane Channel. The scheme of the flow and the system of Cartesian coordinates are presented in Fig. 1. We have two infinite parallel plates, the distance between which is equal to $2h$. The forced flow takes place only in the direction of x. The flow is isothermal and laminar. We ignore the friction of the fluid against the side walls and assume that $B >> h$.

To obtain computational formulas, we will avail ourselves of the Rabinovich–Mooney method [1, 3]. We will write the relationship between the stress τ and shear rate $\dot{\gamma}$ in the form of the equation of state:

$$\dot{\gamma} = f(\tau) . \tag{1}$$

The fluid flow rate and the velocity profile on the assumption of the validity of the condition of fluid adherence to the wall (absence of slip) are determined by the integrals [1, 3]

Volzhsky Polytechnic Institute (branch) of the Volgograd State Technical University, 42 Engels Str., Volzhsky, Volgograd Region, 404121, Russia; email: svm-5@mail.ru, svm24412@gmail.com. Translated from Inzhenerno-Fizicheskii Zhurnal, Vol. 90, No. 5, pp. 1275–1281, September–October, 2017. Original article submitted September 16, 2016.

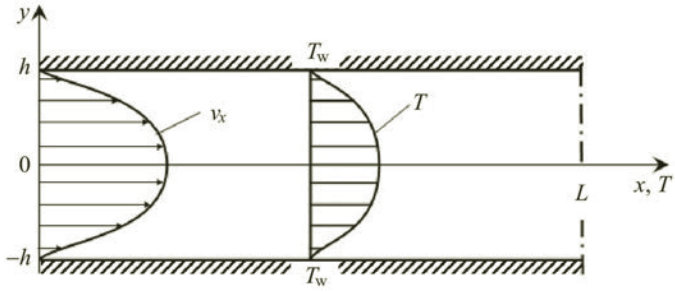

Fig. 1. Computational scheme.

$$\frac{Q}{2Bh^2} = \frac{1}{\tau_w^2}\int_0^{\tau_w} \tau f(\tau) d\tau\,, \quad V(\xi) = \frac{2Bh^2}{Q}\int_\xi^1 f(\tau_w \xi) d\xi\,. \tag{2}$$

Here $\tau_w = h\Delta p/L$, $\tau = \tau_w y/h$, $\xi = y/h$, and $V = 2Bhv_x/Q$.

Let us consider *the Ostwald–de Waele fluid flow*:

$$\tau = \mu_0 \dot{\gamma}^n, \quad f(\tau) = (\tau/\mu_0)^{\frac{1}{n}}\,. \tag{3}$$

Substituting expression (3) into formulas (2) and performing integration, we obtain

$$\frac{Q}{2Bh^2} = \frac{n}{1+2n}\left(\frac{\tau_w}{\mu_0}\right)^{\frac{1}{n}}, \quad V(\xi) = \frac{1+2n}{1+n}\left(1 - \xi^{1+\frac{1}{n}}\right). \tag{4}$$

According to expression (4), the profile of dimensionless velocity at any stress on the wall is determined by the flow index. In the Newtonian case ($n = 1$), we have a parabolic distribution $V(\xi) = 1.5(1 - \xi^2)$.

The Ellis fluid flow. In this case, the equation of state (1) takes the form

$$\dot{\gamma} = f(\tau) = a\tau + b\tau^\alpha\,. \tag{5}$$

Substituting expression (5) into formulas (2), we obtain

$$\frac{Q}{2Bh^2} = \frac{a\tau_w}{3} + \frac{b\tau_w^\alpha}{2+\alpha}, \quad V(\xi) = \frac{\frac{a\tau_w}{2}\left(1-\xi^2\right) + \frac{b\tau_w^\alpha}{1+\alpha}\left(1-\xi^{1+\alpha}\right)}{\frac{a\tau_w}{3} + \frac{b\tau_w^\alpha}{2+\alpha}}\,. \tag{6}$$

According to (6), the dimensionless velocity profile depends not only on the rheological constants of the Ellis model (a, b, α), but also on the shear stress on the wall.

For numerical analysis we will avail ourselves of the data of rheological investigations made in work [4]. Measurements were carried out on a plunger-type capillary viscosimeter. The rubber mixture was used based on SKI-3NT and SKMS-30ARKPN raw rubbers (50 mass parts each), containing technical carbon PM-15 (35 mass parts) and PGM-33 (38 mass parts) as fillers. The main composition also contained straw oil (18 mass parts), sulfur (1.5 mass part), and zinc oxide (3 mass parts). The diameters of the plunger and the cylindrical chamber of thermostating were equal to 9.52 mm, the diameter of the capillary was 2 mm, and the temperature of the mixture in tests was maintained equal to 120°C. The interval of shear stresses from 0.123 to 0.203 MPa was investigated. The expressions $\tau_w = h\Delta p/L$ and $\tau = \tau_w y/h$ allow one to determine pressure and shear stress in megapascals, with the computational equations remaining unchanged.

As a result of the processing of the flow curve by the method of selected points, the following values of rheological constants for the Ellis model have been obtained: $\alpha = 17.893$, $a = 350.217$ MPa^{-1}·s^{-1}, $b = 2.373\cdot10^{15}$ MPa$^{-\alpha}$·s^{-1}. Correspondingly, for the Ostwald–de Waele model we obtained: $n = 0.071$, $\mu_0 = 0.124$ MPa·s$^{0.071}$. The material is a clearly

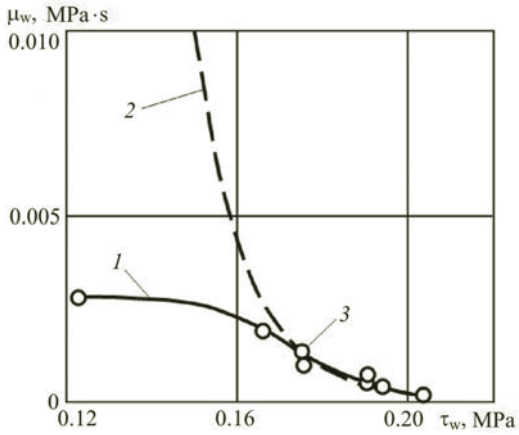

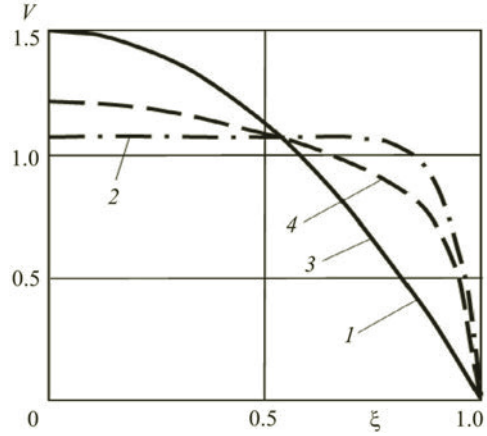

Fig. 2. Viscosities on the wall for the Ellis fluid (1) and Ostwald–de Waele fluid (2) vs. the shear stress on the wall; (3), experimental points.

Fig. 3. Dimensionless velocity profiles in Ostwald–de Waele fluid flow (1, n = 1; 2, 0.071) and in Ellis flow (3, τ_w = 0.123 MPa; 4, 0.202).

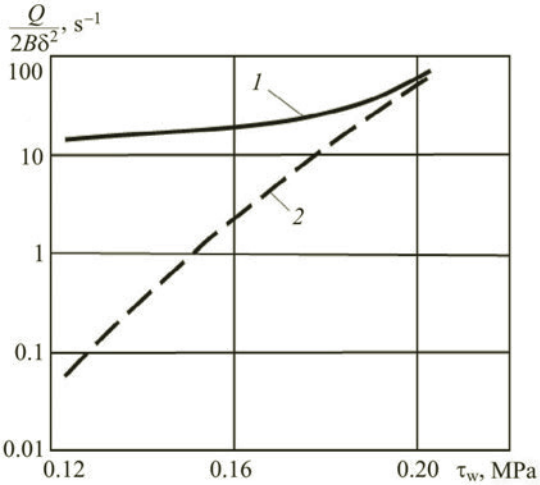

Fig. 4. Flow rate characteristics of Ellis fluid flow (1) and of Ostwald–de Waele fluid flow (2).

expressed pseudoplastic. The processing of rheological data was carried out without account for Weissenberg–Rabinovich′s correction, because it does not exert a qualitative influence on the result.

A comparison of the approximations with experimental points is illustrated with the aid of the dependence of effective viscosity on shear stresses ($\mu_w = \tau_w/\dot{\gamma}$). Since the shear stress is measured in megapascals, the dimensionality of the viscosity will be MPa·s. The expressions for calculating the effective viscosity in the Ellis model (5) and in the Ostwald–de Waele model (3) have the form

$$\mu_w = \left(a + b\tau_w^{\alpha-1}\right)^{-1}, \quad \mu_w = \mu_0 \left(\tau_w/\mu_0\right)^{\frac{n-1}{n}}. \tag{7}$$

The calculated dependences of viscosity on shear stress obtained with the aid of formulas (7) are presented in Fig. 2. It is seen that at high values of shear stresses both models yield closely coinciding results. However, at stresses less than 0.16 MPa, considerable disagreement exists between the predicted viscosities. The Ellis model demonstrates a monotonically varying viscosity and agrees well with experimental results. At the same time, the Ostwald–de Waele model shows an overestimated viscosity, which, in particular, follows from the computational formula (7) (at $n < 1$ for $\tau_w \to 0$ and $\mu_w \to \infty$).

Figure 3 presents the results of numerical analysis of formulas (4) and (6).

The diagram for the Ostwald–de Waele Newtonian fluid ($n = 1$) was plotted for comparison. Curve 2 corresponds to the Ostwald–de Waele fluid for the entire range of shear stresses. In the Ellis fluid flow, the velocity profile depends on the stress on the wall. In the range of low shear stresses, $\tau_w < 0.123$ MPa (low pressure gradients), the velocity profile is close to the Newtonian one (line 3), and lines 1 and 3 practically merge. The non-Newtonian effect (line 4) increases with the shear stress.

It should just be noted that the velocity profile exerts a substantial influence on the intensity of the processes of heat and mass transfer; consequently, the Ostwald–de Waele model is unsuitable for their adequate description.

Figure 4 presents, in semilogarithmic coordinates, the calculated flow rate characteristics of the Ostwald–de Waele (4) and Ellis (6) fluid flows. It is seen from the figure that the power-law model yields substantially underestimated values of the flow rate, especially with decrease in the shear stress. The discrepancy decreases at high shear stresses. The results obtained correlate well with the data on the rheological investigations presented in Fig. 2, according to which the viscosity predicted by the Ostwald–de Waele model increases substantially with decreasing shear stress. Analogous calculations were carried out for polyethylene melt flow in a round channel. The results agree qualitatively with the results presented in this work.

Heat Transfer Problem. During tube flow of polymer melts having a high viscosity there occurs intense heat release due to the internal friction. The intensity of heat release changes from zero in the center of the channel to a maximum value near the channel wall.

We will estimate the error of the power-law model in solving a relatively simple problem of heat transfer. The estimation is carried out by comparing the calculated results for the power-law model with the results for the Ellis fluid. The scheme of flow and thermal loading of a non-Newtonian fluid in a plane slit is presented in Fig. 1. The rheological and thermophysical constants are independent of temperature. The flow is steady-state and laminar. The wall temperature is maintained constant (boundary condition of the first kind). We assume that $\partial/\partial x = \partial/\partial z = \partial/\partial t = 0$. The problem amounts to searching for the temperature distribution in the transverse section so removed from the inlet that the temperature is independent of the longitudinal coordinate.

The temperature field is described by the Fourier–Kirchhoff equation [1] and by the boundary conditions:

$$\lambda \frac{d^2T}{dy^2} + \tau \left(\frac{dv_x}{dy} \right) = 0 , \tag{8}$$

$$y = 0 , \quad \frac{dT}{dy} = 0 , \tag{9}$$

$$y = \pm h , \quad T = T_w . \tag{10}$$

To close problem (8)–(10), one of the following rheological models is used: the Ostwald–de Waele one (3) or the Ellis one (5). The relations obtained earlier, say $\tau = \tau_w y/h$, are taken into account.

As a result of the integration of the Fourier–Kirchhoff equation (8) subject to conditions (9) and (10), for the Ellis model (5) we obtain the following temperature distribution:

$$\theta_E = \frac{a\tau_w^2}{12} \left(1 - \xi^4 \right) + \frac{b\tau_w^{\alpha+1}}{(\alpha + 2)(\alpha + 3)} \left(1 - |\xi|^{\alpha+3} \right) . \tag{11}$$

Correspondingly, for the Ostwald–de Waele model (3) we obtain

$$\theta_{O-W} = \frac{n^2 \tau_w^{1+\frac{1}{n}}}{(1 + 2n)(1 + 3n) \mu_0^{\frac{1}{n}}} \left(1 - |\xi|^{3+\frac{1}{n}} \right) . \tag{12}$$

In expressions (11) and (12) the following notation has been adopted:

$$\theta_E = \frac{(T_E - T_w)\lambda}{h^2} , \quad \theta_{O-W} = \frac{(T_{O-W} - T_w)\lambda}{h^2} , \quad \xi = \frac{y}{h} . \tag{13}$$

The expression for the temperature in formulas (11)–(13) does not involve rheological parameters and provides the possibility for comparing the temperature curve of both models under identical conditions of flow.

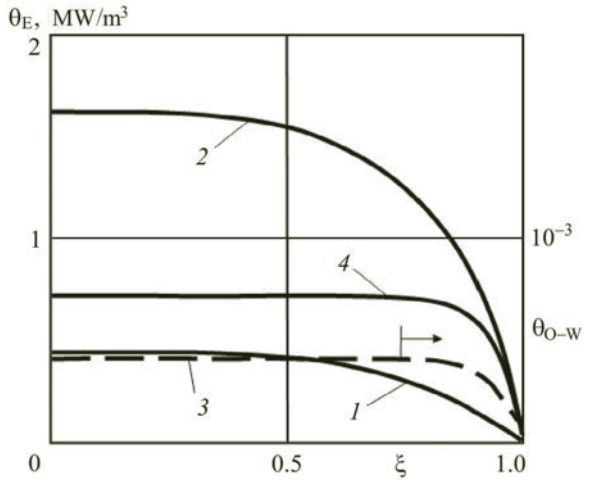

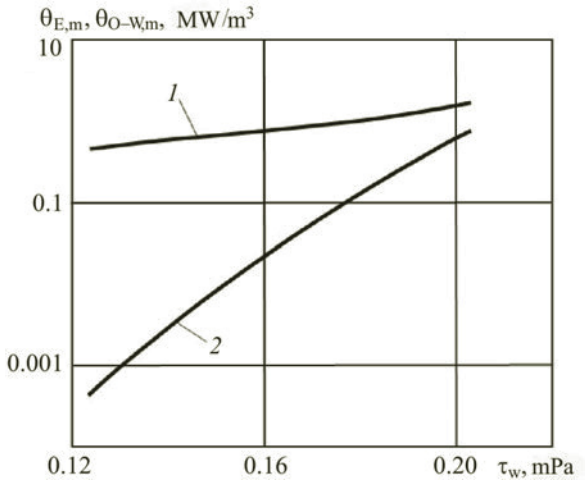

Fig. 5. Temperature distribution in the cross section of the channel with the Ellis fluid flow (1, 2) and the Ostwald–de Waele fluid flow (3, 4): 1, 3, τ_w = 0.123 MPa; 2, 4, 0.203.

Fig. 6. Maximum temperature vs. the shear stress on the wall for the Ellis fluid (1) and Ostwald–de Waele fluid (2).

According to expressions (11) and (12), the temperature profile has maxima at the point $\xi = 0$. In this case, the maximum temperatures for the Ellis model (11) and the Ostwald–de Waele model (12) are described by the expressions

$$\theta_{E,m} = \frac{a\tau_w^2}{12} + \frac{b\tau_w^{\alpha+1}}{(\alpha+2)(\alpha+3)}, \quad \theta_{O-W,m} = \frac{n^2\tau_w^{1+\frac{1}{n}}}{(1+2n)(1+3n)\mu_0^{\frac{1}{n}}}. \tag{14}$$

Here the following designations are used: $\theta_{E,m} = \theta_E(\xi = 0)$, $\theta_{O-W,m} = \theta_{O-W}(\xi = 0)$.

To carry out a numerical analysis, we will avail ourselves of the earlier obtained rheological characteristics. Figure 5 presents the calculated temperature profiles constructed with the use of expressions (11) and (12) for the least shear stress (τ_w = 0.123 MPa) and the highest shear stress (τ_w = 0.203 MPa) on the wall. It is seen that in the case of the Ellis fluid (lines 1, 2) there is a smooth change in the temperature over the entire section. For the Ostwald–de Waele fluid (lines 3, 4), the temperature distribution in the flow core is practically homogeneous and changes sharply near the wall over the portion $0.8 < \xi < 1$. In this case, the shape of the curve is unchangeable, since, according to expression (12), it depends only on the flow index. Moreover, in absolute value, the Ostwald–de Waele model at low stresses on the wall shows substantially underestimated values of temperature (curve 3).

Figure 6 presents the graph of the change of the maximum temperature in the center of the flow with variation of the shear stress on the wall. Use was made of the computational formulas (14). It is seen from the figure that the Ostwald–de Waele model yields highly underestimated values of temperature in the entire range. With decrease in the shear stresses the discrepancy increases, attaining three decimal orders. We also have studied the influence of the shear stress at the wall on the heat flux density on the wall. The graph of the dependence of the heat flux density on the shear stress is analogous to that presented in Fig. 6. The considerable discrepancy is attributed to the inaccurate description of the kinematic characteristic of non-Newtonian fluid flow by the Ostwald–de Waele model, which was noted earlier.

Thus, the power-law model yields a large error in the prediction of the temperature field and in the description of the change in the maximum temperature with the shear stress on the wall. The discrepancy decreases when the flow index approaches unity. It is evident that at other forms of thermal loading too, including nonstationary problems, error in the prediction of the velocity profile will lead to errors in the calculation of the temperature field and heat fluxes.

The power law model can be used for tentative determination of the contour of the plastic core with subsequent application of the viscoelastic model, for example, of the Shvedov–Bingham one.

When a simple shift predominates in flow (for example, the operation of rolls is accompanied by great friction), it is possible to isolate the simple shear component of flow as the predominant one, responsible for the effects of viscosity anomaly, and apply the power law model [5–9]. However, formally an approximate solution of the problem is obtained in such a case.

CONCLUSIONS

1. The error of the prediction by the Ostwald–de Waele model depends on the shape of the cross section of a channel, magnitude of the shear tress on the wall, and on the flow index.
2. The error of the Ostwald–de Waele model in predicting the integral parameters of flow (flow rate, temperature) increases with decrease in the shear stress on the wall.
3. At the given shear stress on the channel wall, the value of the error increases with the deviation of the flow index from unity ($n < 1$).
4. The results obtained should be taken into account in using the Ostwald–de Waele model in heat and mass transfer problems (stationary and nonstationary), for which the accuracy of description of the velocity field is of decisive importance.

NOTATION

a, b, constants of the Ellis model, $MPa^{-1}\cdot s^{-1}$, $MPa^{-\alpha}\cdot s^{-1}$; B, width of the slit, m; $2h$, distance between plates, m; L, channel width, m; n, flow index in Ostwald–de Waele model; Q, volume flow rate of fluid, m^3/s; t, time, s; T, T_w, temperatures of fluid and of the channel wall, K; T_E, T_{O-W}, temperatures of the Ellis fluid and of the Ostwald–de Waele fluid, K; v_x, axial velocity, m/s; V, dimensionless velocity; x, y, z, Cartesian coordinates, m; α, constant in the Ellis model, dimensionless quantity; $\dot{\gamma}$, shear rate, s^{-1}; Δp, pressure fall, MPa; θ_E, θ_{O-W}, temperatures of the Ellis and Ostwald–de Waele fluid flows, MW/m^3; $\theta_{E,m}$, $\theta_{O-W,m}$, maximal temperatures on the axis of the Ellis and Ostwald–de Waele fluid flows, MW/m^3; λ, coefficient of thermal conductivity of fluid, MW/(m·K); μ_0, a constant of the Ostwald–de Waele rheological model, $MPa\cdot s^n$; μ, effective viscosity, MPa·s; ξ, dimensionless transverse coordinate; τ_w, shear stress on the wall, MPa; τ, shear stress, MPa. Indices: w, value on the channel wall; x, along the x axis; E, for the Ellis model; O–W, for the Ostwald–de Waele model; m, maximum temperature.

REFERENCES

1. J. M. McKelvey, *Polymer Processing*, John Wiley & Sons Inc, New York (1962).
2. Z. P. Shul′man, *Convective Heat and Mass Transfer of Rheologically Complex Fluids* [in Russian], Énergiya, Moscow (1975).
3. G. Astarita and G. Marrucci, *Principles of Non-Newtonian Fluid Mechanics*, McGraw-Hill (1974).
4. V. N. Krasovskii, A. M. Voskresenskii, and V. M. Kharchevnikov, *Examples and Problems on the Technology of Processing Elastomers* [in Russian], Khimiya, Leningrad (1984).
5. V. M. Shapovalov, L. M. Beder, and N. V. Tyabin, Flow and heat transfer of an anomalously viscous fluid in the gap between rotating and stationary disks with nonuniform pressure about the perimeter, *J. Eng. Phys. Thermophys*., **49**, No. 5, 1276–1281 (1985).
6. V. M. Shapovalov, Flow of anomalously viscous fluid in a wedge-like gap with elastic wall, in: *Rheology, Processes and Apparatuses of Chemical Technology*, Interinst. Collection of Sci. Papers [in Russian], Izd. "RPK" Politekhnik," Volgograd (2010), pp. 74–77.
7. V. M. Shapovalov, *Roller-Flows of non-Newtonian Fluids* [in Russian], Fizmatlit, Moscow (2011).
8. V. M. Shapovalov, *Processes of Heat and Mass Transfer in Technological Equipment* [in Russian], Izd. Ucheb. Nauch. Lit. Volgogradsk. Gos. Tekh. Univ., Volgograd (2015).
9. V. M. Shapovalov, Application of a polymer compound to a plane surface by an elastic plate, *J. Eng. Phys. Thermophys*., **90**, No. 2, 484–490 (2017).